

# Effects of thermal- and spin- fluctuations on the band structure of purple bronze $\text{Li}_2\text{Mo}_{12}\text{O}_{34}$

T. Jarlborg, P. Chudzinski, and T. Giamarchi

DPMC-MaNEP, University of Geneva, 24 Quai Ernest-Ansermet, CH-1211 Geneva 4, Switzerland

(Dated: February 25, 2013)

The band structures of ordered and thermally disordered  $\text{Li}_2\text{Mo}_{12}\text{O}_{34}$  are calculated by use of ab-initio DFT-LMTO method. The unusual, very 1-dimensional band dispersion obtained in previous band calculations is confirmed for the ordered structure, and the overall band structure agrees reasonably with existing photoemission data. Dispersion and bandstructure perpendicular to the main dispersive direction is obtained. A temperature dependent band broadening is calculated from configurations with thermal disorder of the atomic positions within the unit cell. This leads a band broadening of the two bands at the Fermi energy which can become comparable to their energy separation. The bands are particularly sensitive to in-plane movements of Mo sites far from the Li-sites, where the density-of-states is highest. The latter fact makes the effect of Li vacancies on the two bands relatively small. Spin-polarized band results for the ordered structure show a surprisingly large exchange enhancement on the high DOS Mo sites. Consequences for spin fluctuations associated with a cell doubling along the conducting direction are discussed.

PACS numbers:

## I. INTRODUCTION.

The Lithium Purple Bronze,  $(\text{Li}_{0.9}\text{Mo}_6\text{O}_{17})$  is an unusual material which draws attention of research for nearly three decades [1, 2]. It is a compound with a rather complicated layered structure [3] and highly 1-dimensional (1D) electronic interactions [4–6]. Indeed band calculations with 3D interactions show an electronic structure with 1D character [5, 6], and with large band dispersion in the direction perpendicular to the layers. The band structure shows that two bands are very close together near the crossing of the Fermi energy,  $E_F$ .

Because of its one dimensional electronic properties, the purple bronze is a good playground to study the physics of one-dimensional interacting fermionic systems, which is described by the Tomonaga-Luttinger liquid (TLL) universality class [7]. In fact, several experimental results [8–12] are consistent with the observation of such one-dimensional physics.

However some deviations from the simple TLL scaling are also present. Recent results from angular resolved photoemission spectroscopy (ARPES), done with very high resolution by Wang *et al* [8, 9], indicate some deviations from TLL predictions. The exponents for  $\omega$  and  $T$  dependence are different from predictions from TLL theory, and yet another exponent is deduced from scanning tunnelling measurements (STM) [10].

It is thus important to examine the possible sources from such deviations. One possible origin, as with any quasi-one dimensional system can come from the inter-chain coupling, which drives the system away from the one dimensional fixed point. We determined in another paper, starting from the limit of high energy, a microscopic model incorporating the effects of interactions and hopping between the chains [13]. Such model applicable for energies above 30 meV gives results compatible with a Luttinger liquid description.

In the present paper we focuss on the low energy limit, and examine using Density Functional Theory (DFT) if additional ingredients should be incorporated in this previous description based on a *rigid* band structure for the material. In particular we examine whether the thermal motion of the atoms in the solid can lead to a significant enough source of disorder that could blur the 1D description. Such effects, in three dimension, are indeed important for the properties of certain classes of compounds with sharp structures of the density-of-states (DOS) near  $E_F$ , such as in the B20 compound FeSi [14], and also for the appearance of the bands in other materials [15–17].

We thus reexamine, in this light, in the present paper the band structure of the purple bronze. In order to ascertain the effects of the perpendicular hopping we compute carefully the dispersion in the transverse direction. In addition we examine the effects of thermal fluctuations and spin fluctuations.

The plan of the paper is as follows. In Sec. II we describe the method with the results for ordered structure. The effect of deviations from the ideal atomic structure, due e.g. from thermal fluctuations, are given in Sec. III. Section Sec. IV is dedicated to the effects of static, substitutional disorder. Results for spin fluctuations and a discussion of their effects are given in Sec. V. In Sec. VI we present models of how smearing and partial gaps can modify photoemission intensities.

## II. BAND STRUCTURE.

In this section we apply density functional band theory (DFT) in order to see to what extent it can explain the unusual photoemission data. In doing so it is important to note that effects of thermal disorder and spin-fluctuations may be important and have to be included in the density functional approach. The electronic struc-

ture of  $\text{Li}_2\text{Mo}_{12}\text{O}_{34}$  (two formula units of stoichiometric purple bronze) has been calculated using the Linear Muffin-Tin Method (LMTO, [18, 19]) in the local density approximation [20](LDA), with special attention to effects of structural disorder. The lattice dimension and atomic positions of the structure have been taken from Onoda *et al* [3]. The lattice constant in the conducting  $y$ -direction,  $b_0$ , is 5.52 Å and more than two times larger along the least conducting  $x$ -direction  $a_0 = 12.76$  Å. Thus the structure consist of well separated slabs. In order to adapt the LMTO basis for an open structure as purple bronze we inserted 56 empty spheres in the most open parts of the structure. This makes totally 104 sites within the unit cell. The basis consists of s,p- and d-waves for Mo, and s- and p-states for Li, O and empty spheres, with one  $\ell$  higher for the 3-center terms. Corrections for the overlapping atomic spheres are included. All atomic sites are assumed to be fully occupied (except for the case with a vacant Li atom, see section Sec.IV), and they are all considered as inequivalent in the calculations. Self-consistency is made using 125 k-points, with more points for selected paths for the band plots.

The band structure for the undistorted structure is shown in Figs. 1-3. The total DOS at  $E_F$ ,  $N(E_F)$ , is not very large, 2.1 states per cell and eV. The states at  $E_F$  are mainly of Mo-d character coming from sites far from the region containing Li, where locally  $N(E_F)$  amounts to about 0.2 st./eV/Mo. This is less than 1/3 of  $N(E_F)$  in bcc Mo.

Two bands, number 139 and 140 (counted from the lowest of the valence bands), are the only ones crossing  $E_F$ . It was already pointed out in Ref.[5] that these two bands originate from zig-zag chains (oriented along  $y$ -axis) which are grouped in pairs (along  $z$ -axis). This is the way each structural slab is built. The two bands have similar DOS at  $E_F$  to within 10 percent accuracy. The Fermi velocity,  $v_F^y$ , along the conducting  $y$ -direction is normal as for a good metal, about  $5 \cdot 10^5$  m/s, but the ratio between the Fermi velocity in  $y$ - and  $z$ -directions, about 50, is compatible with the reported anisotropic 1D-like resistivity [4]. The velocity along  $\vec{x}$  is even smaller [21]. The bands and the DOS agree reasonably with the bands calculated by Whangbo and Canadell [5] and Popović and Satpathy [6] using different DFT methods. In Figs. 2-3 we show the details of the bands near  $E_F$ , where the band separation and the electronic interactions (or  $t$ -integrals in a tight-binding language) can be extracted. The band dispersion along the conducting the  $\Gamma - Y$  (or  $P - K$ ) direction agree well with the measured results obtained by ARPES [9] showing a flattening of the two dispersive bands at about 0.4-0.5 eV below  $E_F$ . Other bands are found about 0.25 eV below  $E_F$ . The calculated structures A,B,C and D are identified on the bands in the  $P - K$  direction in Fig. 2 at 0.6 (0.6), 0.4 (0.3), 0.6 (0.5) and 0.5 (0.4) eV below  $E_F$ , respectively, where the values within parentheses are taken from the photoemission data of Ref. 9. Thus, there is an upward shift of the order 0.1 eV in photoemission compared to

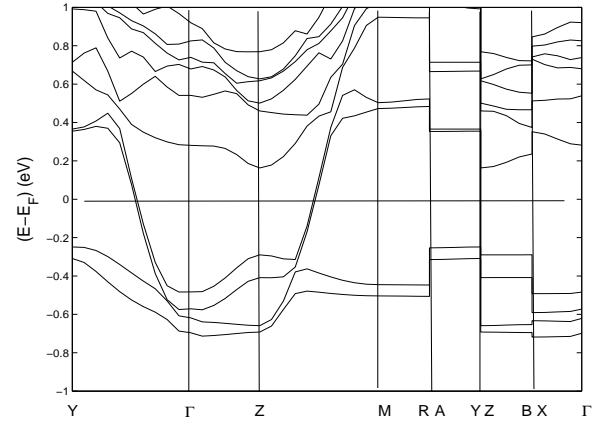


FIG. 1: Band structure of of purple bronze  $\text{Li}_2\text{Mo}_{12}\text{O}_{34}$  computed within DFT-LDA approximation for the rigid structure with parameters taken from Ref.[3]. Bands are shown along symmetry lines in a 1eV window around the Fermi energy  $E_F$ .

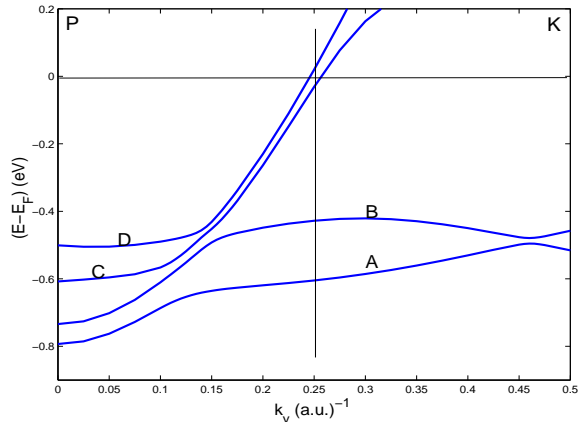


FIG. 2: Band dispersion along  $PK$  (parallel to  $\Gamma - Y$  halfway inside the zone) showing that Fermi momentum  $k_F$  is very close to half of the  $P - K$  distance (at the vertical line). The two bands crossing  $E - F$  are very close for momenta just below  $k_F$  (for details see Fig.3) but they are separated by  $\sim 100$  meV for  $|k| \leq \frac{1}{2}|k_F|$ . chosen because the separation between the two bands (C and D) is the largest for this value of  $k_z$ . Notation as in Ref.[9]; C and D corresponds to bands 139 and 140 respectively.

the calculated bands. Such trends are typical, for instance in ARPES on the cuprates, and can to some extent be attributed to electron-hole interaction in the excitation process [22]. The overall agreement between different band results and photoemission is reassuring for this complicated structure, while we now should focus on finer details of the bands near  $E_F$ .

The 1-D character of the band structure is revealed from the comparison between Figs. 1-3. While the band width for the bands crossing  $E_F$  is of the order 2 eV

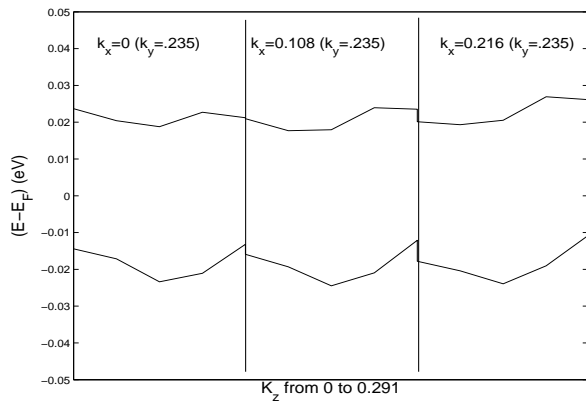


FIG. 3: Band dispersion of the two bands crossing  $E_F$  shown along the second conducting  $z$ -direction. Because of lattice symmetry only a half of a dispersion curve ( $k$ -values in units of  $2\pi/b_0$ ) is shown. Three different cuts of relevant portions of the Brillouin zone are given.

in the  $y$ -direction, it is not larger than 0.02 eV along  $z$  and  $x$ . These low values and the shape of the  $z$ - and  $x$ -dispersions are of importance for a Luttinger description of bands close to  $E_F$  [13]. It should be noted that the in-plane band dispersion is very small, and that the 2 bands have similar but not identical shapes along the  $z$ -direction, see Fig. 3. The dispersion is quite unusual with minimum in the middle of the Brillouin zone instead at  $q_c = 0$ . This suggests that there exist not only one but several equally important, competing hybridization paths between different chains. A brief analysis of the structure[21] indicates that several paths are possible. First, for the closest pair of zig-zag chains there is a direct hopping between Mo(1) and Mo(4) sites, and an indirect one going through Mo(2) and Mo(5) atoms. Secondly, the hopping between these pairs (of chains) always has to go through Mo(2) atoms, while the next nearest neighbor hopping goes through M(2) and M(5) atoms.

The direct inter-chain hopping (between Mo(1) and Mo(4) sites) is weakened because it goes through rather weak  $\delta$ -bond, while hoppings through M(2) and M(5) sites are enhanced because their octahedra are more distorted. The cuts along different  $k_b$  are nearly identical, which shows that this competition does not depend on the momentum of the propagating wavepacket. The amplitude of the inter-chain hopping, as computed from band structure shows that the one dimensionality of the compound is certain for energies above  $\sim 20$  meV, scale of the bare inter-chain coupling. Below this energy the question is open, and will be strongly dependent on how the transverse hopping can be affected by strong correlations [13].

Another check was also made by calculating the bands for the structural  $a$ -,  $b$ -, and  $c$ -parameters corresponding to low  $T$ . It has been reported that the thermal expansion is quite unusual, where almost no expansions are

found along  $b$  and  $c$  between 0 K up to room temperature [23, 24]. A calculation for the ordered structure with all structural  $a$ -parameters downscaled by 0.3 percent, to correspond to the structure at 0 K, was made. The effects on the bands are very small and not important for the properties discussed in this work. The average band separation decreases, but the change is not significant compared to the original band separation of the order of 30 meV.

### III. THERMAL DISORDER AND ZERO-POINT MOTION.

The previous results were obtained by assuming an ideal periodic structure. Band structure calculations rarely take into account thermal distortions of the lattice positions. However, structural disorder due to thermal vibrations is important at high  $T$ , and properties for materials with particular fine structures in the DOS near  $E_F$  may even be affected at low  $T$  [14, 25]. Here for purple bronze, effects of thermal fluctuations might be pertinent on the degree of dimensionality, the band overlap between the two bands at  $E_F$ .

Phonons are excited thermally following the Bose-Einstein occupation of the phonon density-of-states (DOS),  $F(\omega)$ . The averaged atomic displacement amplitude,  $\sigma$ , can be calculated as function of  $T$  [26, 27]. The result is approximately that  $\sigma_Z^2 \rightarrow 3\hbar\omega_D/2K$  at low  $T$  due to zero point motion (ZPM) and  $\sigma_T^2 \rightarrow 3k_B T/K$  at high  $T$  (“thermal excitations”), where  $\omega_D$  is a weighted average of  $F(\omega)$ . The force constant,  $K = M_A\omega^2$ , where  $M_A$  is an atomic mass (here the mass of Mo is used because of its dominant role in the DOS), can be calculated as  $K = d^2E/du^2$  ( $E$  is the total energy), or it can be taken from experiment. We use the measurements of the phonon DOS of the related blue bronze  $K_{0.3}MoO_3$  [28] to estimate  $K$  and the average displacements of Mo atoms, as will be explained later.

The individual displacements  $u$  follow a Gaussian distribution function.

$$g(u) = \left(\frac{1}{2\pi\sigma^2}\right)^{3/2} \exp(-u^2/2\sigma^2) \quad (1)$$

where  $\sigma$ , the standard deviation, will be a parameter in the different sets of calculations. In order to get an estimate to the effect of such atomic displacements on the band structure, each atomic site in the unit cell is assigned a random displacement along  $x$ ,  $y$  and  $z$  following the Gaussian distribution function. Band calculations are made for a total of nine different disordered configurations. The effects will be a shift of the band position, to which both ZPM and thermal fluctuations contribute and a broadening of the bands. Our calculation, in which we will displace atoms from their natural position, will also give information on the nature of the band, and their sensitivity in touching a certain type of atoms.

For these investigations we have performed two types of simulations of thermal effects: first including all atoms

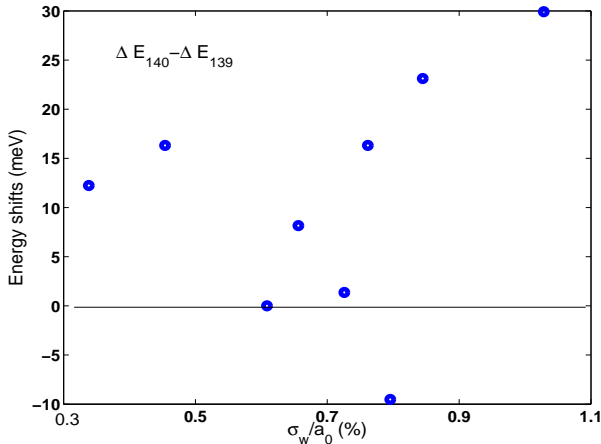


FIG. 4: The difference of average shifts of the two bands between ordered and disordered structures as function of the site weighted disorder parameter  $\sigma_w$ . The zero-point motion corresponds approximately to  $\sigma_w$  lower than 0.7 means that the two bands move closer for that disorder. Band broadening in the case for  $\sigma_w \approx 0.7$ , when there is no significant average shift, is only because of internal wiggling of the bands, see fig. 5.

(treated on equal footing) and second only for atoms around the zig-zag chain where the DOS at  $E_F$  is high. In the latter case, the distortion,  $\sigma_w$ , is averaged over those sites only, see later. These calculations confirm, as expected from the static band structure, that mostly atoms around the zig-zag chains contributes to observed effects. No general correlation between the displacements of nearest neighbors is taken into account, but extreme values of  $u$  are limited in order to avoid that two atomic spheres make a “head-on” collision, which of course would not occur in the real material. Further refinements of the disorder could involve different disorder for different atomic mass, and anisotropic disorder. Purple bronze is a layered material, 1D-like, and it is probable that vibrational amplitudes are different perpendicular to the planes compared to within the layers. However, such information is missing and here we assume equal isotropic disorder for all atom types. The present calculation already gives an estimate of the typical effects of such atomic displacements.

The broadening parameter  $\sigma$  depends on  $T$  and the properties of the material. From the experimental data in blue bronze [28] we estimate the  $T$ -dependence of  $\sigma$  for purple bronze. From this we find that  $\sigma_Z/b_0$  is of the order 0.7 percent for Mo, and thermal vibrations become larger than  $\sigma_Z$  from about 120 K. For oxygen sites  $\sigma_Z/b_0$  is of the order 1 percent. However, as will be discussed later the band structure is more sensitive to disorder on the Mo sites.

Two measures of the band disorder are shown in Figs. 4-5 as function of the weighted displacements,  $\sigma_w$ , calculated as the average of distortions for the 22 sites (far from Li) with the highest  $N(E_F)$ . The broadening

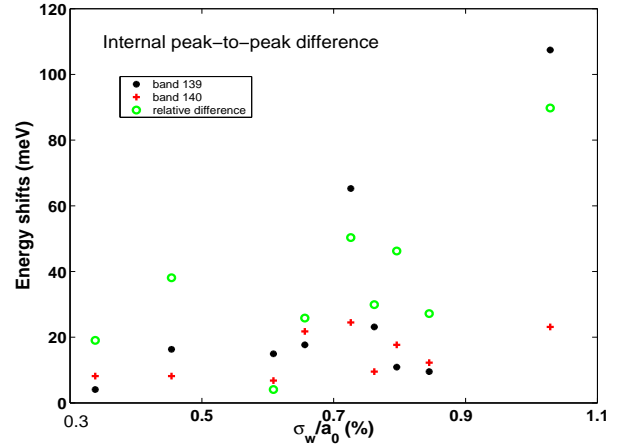


FIG. 5: Internal peak-to-peak energy difference between undistorted and distorted bands (black \* band 139, red + band 140). The green circles show the maximal difference between the two previous values. The site weighted disorder parameter  $\sigma_w$  is defined in the text.

for each of the two bands is calculated from the changes in band energies ( $\epsilon(k)$ ) at 25 k-points, which are found within  $\sim 20$  meV from  $E_F$  in the undistorted case. The difference between average energy shifts of the two bands are shown in Fig. 4 as function of  $\sigma_w$ . This can be thought as a good measure of the thermally induced effects. There are more often positive energy differences, indicating that in average the two bands tend to separate because of the atoms’ random displacements. The net effect is rather weak, we predict only 10 meV difference between room and helium temperature, but it could be observable. What is more the thermal expansion of the crystal in b-direction in anomalously weak, so it should not affect the above result. This outcome is quite unusual, but the origin of it becomes clear when one analyze the structure of a crystal. It has been suggested [5] that  $t_{\perp}$  hopping along c-axis is particularly weak in purple bronze because of certain cancellation in hopping integrals (the  $\delta$ -bonds mentioned in Sec.II), when the ions reside in a high symmetry points. Our finding puts that statement on firm ground: we clearly notice that when ions are slightly shifted the perpendicular hopping can benefit noticeably.

We can gain even more information when studying the internal behavior of the two bands separately. Measures of the “wiggling” of each band because of disorder are displayed in Fig. 5. Peak-to-peak differences are given by

$$\Delta E_{max}^j = |\max[\Delta\epsilon^j(k_n)] - \min[\Delta\epsilon^j(k_n)]|$$

$j = 139$  or  $140$ , where  $\Delta\epsilon^j(k_n)$  is the deviation in energy (with respect to undistorted band) at a certain point  $k_n$  for band  $j$ . The search for extremes goes through the set of k-points  $k_n$  ( $n = [1, 25]$ ). These differences of extremes are shown for the two bands. For the largest disorder, band 139 has changed some 100 meV at one

k-point relative to the change of the same band at some other k-point, however this quite large value has to be taken with caution. In general the bands' wiggling is of the same order as the average difference between the two bands (shown on Fig. 4). We suspect that the origin of wiggling is the same as the origin of increased band separation, namely the activation of certain overlap integrals. However, the fact that the wiggling is equally strong as the band splitting implies, at least within naive tight-binding interpretation, that either the inter-ladder hopping is equally strong or that the next nearest neighbor hopping is of the same order as the standard  $t_{\perp}$ . This second implication goes along the same lines than the ones discussed in the context of Fig. 3.

The lower band appears to be more sensitive than the upper band in this respect. In Fig. 5 is also shown the maximum difference,

$$\Delta\varepsilon = \max|\Delta\epsilon^{139}(k_n) - \Delta\epsilon^{140}(k_n)|$$

It is defined as relative bands deviations at a certain point  $k_n$ . In particular case when the two bands would change in the same way because of thermal disorder (*e.g.* shift homogeneously), then this last value would be equal to the absolute value of what is shown in Fig. 4. This is not the case, which means that the two bands will change quite independently of each other. In other words, most of the k-points are concerned by the energy changes, and the wiggling of the two bands is different. The interpretation of this subtle difference, not visible within standard DFT band structure result, is quite difficult. It implies that bands 139 and 140 do not have identical site dependence. In other words one should not naively assume that they originate from two zig-zag chains which are very weakly hybridized as it is commonly done in the literature. The microscopic complexity of effective interactions, at least at the lowest energy scales of order  $\sim 10\text{meV}$ , needs to be rich.

In our calculation we have considered displacements of all sites, but the bands at  $E_F$  are mostly sensitive to disorder of Mo sites with a high DOS. This is reflected by calculations in which *only* the four Mo with the highest DOS are displaced 0.7 percent of  $b_0$  in a few selected directions. When these sites are displaced perpendicular to the diagonal  $(\vec{x}, \vec{z})$ -direction the average band shift (equivalent to the shifts displayed in Fig. 4 for general disorder) is about 10 meV, while if the displacement is in the directions parallel to the diagonal the shift is about 50 meV. The effect of movements in the  $\vec{y}$ -directions is typically one order of magnitude smaller. This indicates that the phonon mode whose displacements are in the plane perpendicular to zig-zag planes with the movements in the direction of the closest Mo neighbors, is particularly strongly coupled to electronic liquid.

These values of energy changes can be compared with the distance between the bands near  $E_F$  in the undistorted case, shown above in Fig. 3 for the relevant paths in k-space. The undistorted bands are separated by 30-40 meV, and the two bands are confined within 10-15

meV along  $k_x$  and  $k_z$ . The additional wiggling for distorted cases is of the same order, 20-40 meV, as seen in Fig. 5. However, this effect coexists with a small increase of the band separation. The band separation, will generally increase when thermal fluctuations are at play. This is an indication of increased electronic delocalization within the layers towards a more 3D band structure, but this also indicates that any disorder will strongly affect carriers propagation along c-axis. As the temperature increases the thermal fluctuation effects will increase which means that, if this picture is valid, the experimentally observed band broadening should noticeably increase with temperature. This becomes specially important when thermal activation of phonons becomes dominant at about 120 K. In addition, the relatively rapid dispersion along  $k_y$  makes the band overlap important in k-space. For instance, a band separation of 25 meV corresponds to a shift of  $k_y$  of only 0.01 of the  $\Gamma - Y$  distance.

#### IV. STATIC DISORDER

In addition to the thermal effects, on which we concentrated in the previous section, atomic distortions can come from a variety of other sources. In particular imperfections of the crystal (from non-stoichiometry, vacancies, site exchange etc.) should also contribute to the effect. One can also worry about the fact that one out of ten Li atoms are missing in the real material. The unit cell considered here contains two Li, and the influence on the electronic bands from the replacement of one of these with an empty sphere (without taking structural distortion into account) is moderately large. The Fermi level goes down because one electron is removed, but if one neglects the chemical potential shift he finds an increase of the average band separation between band 139 and 140 by about 40 meV. This is comparable with largest calculated effects of thermal disorder, see Fig. 4. However, a more realistic estimate is obtained in virtual crystal calculations where one of the Li is replaced by a virtual atom with nuclear and electron charges of 2.8 (instead of 3.0 for the other Li). This set-up has the correct electron count corresponding to 90 percent occupation of Li. Now the average shifts of the two bands is much smaller, and the wiggling of the bands are not even comparable ( $\sim$  less than half) to what is found from ZPM. Therefore it can be expected that effects from thermal disorder will overcome those from structural disorder in high quality samples.

The smallness of this effect has important implications if one looks from the 1D Luttinger liquid perspective. The random Li vacancies are placed relatively far from zig-zag chains where 1D liquid resides. This implies that interaction will have Coulomb character, the small momentum exchange events shall dominate. Thus substitutional disorder will have primarily forward scattering character with an amplitude  $\approx 15\text{meV}$  as determined

above. This situation can be modelled as a Luttinger liquid with forward disorder. In this case the spectral function is can be given [13]. This implies that substitutional disorder cannot be invoked to explain phenomena taking place at energy scales larger than 15 meV. For these larger energies the standard Luttinger liquid behavior is expected.

## V. SPIN FLUCTUATIONS.

In Figs. 1 and 2 it is seen that the two free-electron like bands cross  $E_F$  very close to half of the  $\Gamma - Y$ - or  $P - K$ -distance along the conducting  $\vec{y}$ -direction of the structure. A doubling of the real space periodicity in this direction would open a gap in the DOS near  $E_F$  and lead to a gain in total energy [29–32], suggesting that this material might have intrinsic spin density waves type instabilities. In strongly correlated materials solving these question is of course complicated, specially in a low dimensional material, since the proper spin exchanges and quantum fluctuations have to be taken into account. Some of these issues can be addressed at the level of the microscopic model derived in Ref. 13. Here we look at the possibility of such a spin instability, at the band structure level and low temperatures, where the two- and three- dimensional aspects of the system can a priori play a more important role, and thus the effect of interactions can be reduced [7].

A complete verification of how a cell doubling with phonons or magnetic waves affects the band near  $E_F$  would require more complex band calculations, and will be a demanding undertaking. Instead we propose at this stage to extract information from calculations for the 104-site cell, and to apply a free electron model of the band dispersion in the  $y$ -direction to see if at all magnetic fluctuations might be of interest for a band gap. We noted that displacements of some Mo with the highest local  $N(E_F)$  contribute much to the band distortion. But the size of the potential shifts at these sites are limited by rather conservative force constants. Therefore, even if a selected phonon can contribute to a gap near  $E_F$ , it might be more effective to open gaps through spin waves since the potential shifts in this case can diverge near a magnetic instability. In order to estimate the strength of the exchange enhancement on Mo we extend our calculations for the ordered structure to be spin polarized with an anti-ferromagnetic spin arrangement of the moments on the Mo with the highest  $N(E_F)$ . This is made by application of positive of negative magnetic fields within the atomic spheres of two groups of four Mo in the cell with the highest DOS.

The propensity for fluctuations of anti-ferromagnetic moments within the cell is surprisingly large according to the calculations. The local exchange enhancement on Mo, corresponding to the Stoner factor for ferromagnetism (i.e. the ratio between exchange splitting and applied magnetic field), is close to 4.5 in calculations at

low field and temperature. The total energy  $E(m)$  is fitted to a harmonic expansion of the moment amplitude  $m$ ,  $E_m = K_m m^2$ , where  $K_m$  is the “force constant”. In analogy with phonon displacement amplitudes one can estimate  $m^2 = k_B T / K_m$  as a measure of the amplitude of moment fluctuations [33]. While phonon distortions  $u$  always increase with  $T$ , in a Fermi liquid framework one expects that magnetic moments  $m$  will be quenched at a certain  $T$  [29]. This is because of a self-supporting process where  $m$  is a function of the exchange splitting  $\xi$ . The latter depends on  $m$  and the local spin density, and the mixing of states above and below  $E_F$  given by the Fermi-Dirac function will reduce  $m$  at high  $T$ , so  $m$  and  $\xi$  can drop quite suddenly. Calculations at an electronic temperature of 200K make  $K_m \approx 2eV/\mu_B^2$ . From this one can estimate that  $m$  will be of the order  $0.1 \mu_B$  per Mo at room temperature corresponds to  $\xi \approx 0.2eV$ . Another complication is that the thermal disorder of the lattice are mixing states across  $E_F$  too, and this is another diminishing factor for spin polarization. Nevertheless, it suggests that spin fluctuations can play a role at low or intermediate temperatures. It is interesting to note that the value of  $\xi$  is of the same order of magnitude than the superexchange parameter calculated from the strong correlations perspective [13, 34]. If one compares this value with the previously determined strength of disorder and effects of thermal fluctuations, one would realize that spin fluctuations play a much more prominent role in the low energy physics. Such fluctuations can potentially lead to pseudogap features in the band dispersion, thus understanding better their properties is an interesting challenge, clearly going way beyond the scope of this paper. On the experimental side, there was only one report of such large gap ( $\Delta > 10meV$ ) in the low energy spectrum [11] and in the light of more recent experiments [12] done with the same method this finding is highly controversial. An extremely small gap has been observed in transport experiments [35], and probably in STM [10], however the spin sector probed by static susceptibility [4, 36] and muon spectroscopy [37] certainly is not gapped. Further theoretical studies are necessary to understand this situation, where high magnetic propensity does not lead to a gap for spin excitations.

## VI. COMPARISON WITH ARPES

We show in this section some of the consequences of the band structure calculated above for the ARPES data. Note that the above calculation do not take into account the effects of strong correlations. Thus the deviations from the picture presented below should thus be direct measure and consequence of such effects. This will of course depend on the range of temperature and/or energy.

In order to simulate ARPES intensities for the free-electron bands near  $E_F$  we ignore matrix elements and energy relaxations due to electron-hole interaction. We

consider one-particle excitations directly from the band occupied according to the Fermi-Dirac distribution, and with pyramidal broadening functions for energy (experimental and intrinsic broadening due to disorder) and momentum,  $k$ . The experimental broadenings have the same FWHM values as in the work of Wang *et al*, and we chose to show cuts in momentum of the same step size as in their work [9]. The free electron band is fitted to the LMTO results so that  $E_F$  is 0.6 eV at  $k_F$ . The splitting into two bands of  $\sim 30$  meV, is assumed constant everywhere, which is approximately true for the real bands near  $E_F$ . A linear background is added to the intensities in order to make a more realistic display of photoemission with secondary excitations. Five cuts in momentum below  $k_F$ , in equal steps as in Ref. 9, descend to about -0.2 eV. The five cuts appear almost equally spaced in energy, since the dispersion is almost linear within the narrow energy interval.

First, as shown in Fig. 6 the band splitting of about 30 meV should be visible in the ARPES data if only the experimental broadening functions were at work. Secondly, the broken lines in Fig. 7 show wider distributions, because of additional broadening coming from the thermal disorder of the lattice. These distributions are not as wide as in Ref. [9]. This strongly suggests that other physical effects (effects of interactions, static disorder due to non-stoichiometry, spin fluctuations) are at play.

As an extreme case we can consider a cell doubling (e.g. due to spin ordering) which would create a gap near  $k_y = k_F$ . The full lines in Fig. 7 show what would happen to the spectra if  $\xi$  in the free-electron model goes up to about 70 meV. In this case it is seen that the band retracts from  $E_F$ , since the peaks for  $k$  closest to  $k_F$  are lower in energy than the broken lines. Far below  $E_F$  there is not much difference between full and broken lines. In the end the presence of a gap leads to a more non-uniform energy distribution of the five  $k$ -cuts of the intensity. Comparison of the experimental features, with the one obtained by such a band structure analysis could thus be useful to investigate the low energy properties of purple bronze, and in particular the existence of a gap or pseudogap in the dispersion relation. The analysis in Ref. [9] revealed a  $T^{0.6}$  scaling of the intensity near  $E_F$  over a wide  $T$ -interval. Ascertaining whether this behavior at low energy comes from one dimensional fluctuations or some pseudogap regime is an important question.

## VII. CONCLUSION.

In this paper we have reexamined the band structure of purple bronze in the ordered lattice and found that the main features of the bands agree well with previous calculations and ARPES results. In particular, only two bands cross the Fermi level. In our study we focus on these two bands. The perpendicular interactions along  $z$  and  $x$  (“perpendicular hoppings”) are weak and ap-

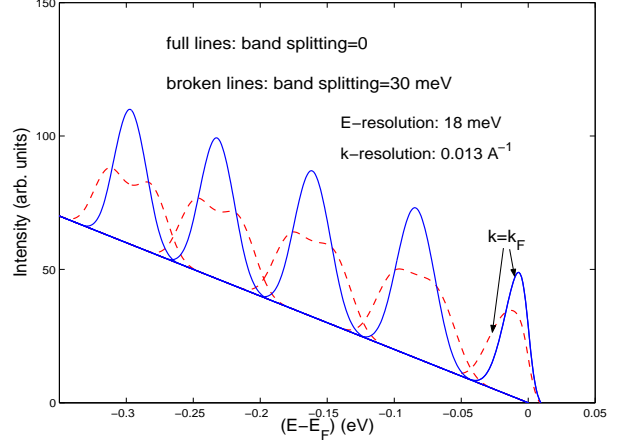


FIG. 6: Free electron intensities for 5  $k$ -values going from  $k_F$  in steps of 3.6 percent of  $\Gamma - Y$  added to an arbitrarily chosen background. The energy and momentum resolutions  $\Delta E$  and  $\Delta k$  are similar to the experimental values in ref. [9]. It is seen that a band splitting of more than  $\sim 30$  meV should be seen in photoemission.

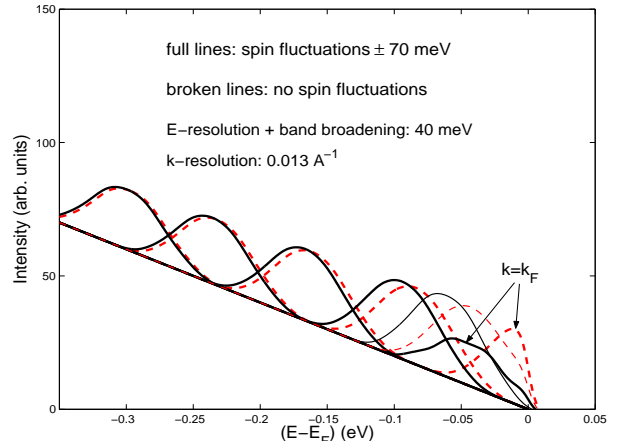


FIG. 7: Calculated intensities for a band splitting of 30 meV as in fig. 6, but where an band broadening from ZPM of  $\sim 25$  meV has been included (broken lines). One intermediate cut with  $k$  at 1.8 percent from  $k_F$  is added in this figure. The band broadening makes the band splitting undetected. Full lines: Including spin fluctuations as described in the text. Note the energy lowering close to  $E_F$ .

pear to lay out the conditions of TLL-like behavior of the bands near  $E_F$ , for energy down to at least 20 meV.

We have investigated whether additional effects, giving small energy distortions at these energy scales could cause an overlap between these two bands at low  $T$ . The energy separation between the two essentially one dimensional bands increases below  $E_F$ , as can be seen in Fig. 1 along the  $\Gamma - Y$  direction. For instance, the two considered bands are separated  $\sim 0.1$  eV at 0.4 eV below  $E_F$ , similarly to what is seen in ARPES at this energy [9]. When bands are closer to  $E_F$  then they are also

closer together, however as shown in Sec.VI within single particle picture (LDA-DFT) they should be distinguishable at low  $T$  provided that intrinsic disorder is not too large and if the matrix elements for transitions from both bands are comparable [38]. As  $T$  increases beyond  $\sim 120$  K or more, the band broadening increases because of additional thermal disorder so that the two bands seem to merge. We find that the thermal effects can potentially play a role in the band separations however one has to keep in mind the temperature dependence of the effect: the bands becomes less and less distinguishable as the temperature increases. There is obviously a complicated cooperation between increase in splitting and wiggling but in any case the following effect can be used to verify experimentally this picture: as the temperature increases the ARPES lines should become noticeably thicker.

Additional calculations for Li deficient purple bronze show no important modifications of the bands crossing  $E_F$ , at least as long as it is not associated with static disorder. Likewise the band structure for a unit cell with modified  $x/y$ - and  $x/z$ -ratios, appropriate for the structure at room temperature, is not very different from what is shown in Fig. 1.

Recent photoemission result of Wang *et al* [9], made at low  $T$ , only detects one band at  $E_F$ . The interpretation of these result is still an exciting issue given the fact that electron-electron interactions can also suppress tunnelling and reinforce the one dimensionality of the material [13]. What we showed in this paper is that at a one body level, the effect of distortion of the electronic

structure, also go in the direction of a smearing of the difference between the two bands and thickening observed ARPES spectra. Disentangling the two effects is thus an important question, and can potentially be done by comparing the predicted band separations, at the level of band structure, with the actual ARPES data.

We have also explored the possibility of anti-ferromagnetic spin fluctuations. Here, our investigations are not complete, but our first results show surprisingly large anti-ferromagnetic exchange enhancements on Mo within the basic unit cell. This and other facts motivate further studies of fluctuations within larger cells, in order to see if they can lead to gap or pseudogap features near  $E_F$ .

It is interesting to note that the existence of thermal fluctuations and imperfections of the atomic structure, makes – at the band structure level – the system more three dimensional. This effect will be in competitions with the renormalization of the inter-chain hopping coming from the electron-electron correlations. The competition between these two effects leads to an intermediate and low temperature physics which is still mysterious in this compound.

Acknowledgments: We would like to thank Jim Allen and Enric Canadell for sharing their knowledge about purple bronze with us. We also acknowledge an additional insight provided by Sachi Satpathy, Tanusri Saha-Dasgupta and Maurits W. Haverkort. This work was supported by the Swiss NSF under MaNEP and Division II.

- 
- [1] W.H. McCarroll and M. Greenblatt, *J. Solid State Chem.* **54**, 282, (1984).
- [2] C. Schlenker, H. Schwenk, C. Escribe-Filippini, and J. Marcus, *Physica* **B135**, 511, (1985).
- [3] M. Onoda, K. Toriumi, Y. Matsuda and M. Sato, *J. Solid State Chem.* **66**, 163, (1987).
- [4] M. Greenblatt, W.H. McCarroll, R. Neifeld, M. Croft and J.V. Waszczak, *Solid State Commun.* **51**, 671, (1984).
- [5] M.-H. Whangbo and E. Canadell, *J. Am. Chem. Soc.* **110**, 358, (1988).
- [6] Z.S. Popović and S. Satpathy, *Phys. Rev. B* **74**, 045117, (2006).
- [7] T. Giamarchi, "Quantum physics in one dimension" (Oxford University Press, Oxford, 2004).
- [8] F. Wang, J.V. Alvarez, S.-K. Mo, J.W. Allen, G.H. Gweon, J. He, R. Jin, D. Mandrus and H. Höchst, *Phys. Rev. Lett.* **96**, 196403, (2006).
- [9] F. Wang, J.V. Alvarez, J.W. Allen, S.-K. Mo, J. He, R. Jin, D. Mandrus and H. Höchst, *Phys. Rev. Lett.* **103**, 136401, (2009).
- [10] J. Hager, R. Matzdorf, J. He, R. Jin, D. Mandrus, M.A. Cazalilla and E.W. Plummer, *Phys. Rev. Lett.* **95**, 186402, (2005).
- [11] J. Xue, L.C. Duda, K.E. Smith, A. V. Fedorov, P.D. Johnson, S.L. Hulbert, W. McCarroll and M. Greenblatt, *Phys. Rev. Lett.* **83**, 1235, (1999).
- [12] G.H. Gweon, J.D. Denlinger, J.W. Allen, C.G. Olson, H. Höchst, J. Marcus and C. Schlenker, *Phys. Rev. Lett.* **85**, 3985, (2000).
- [13] P. Chudzinski, T. Jarlborg and T. Giamarchi, (unpublished 2012).
- [14] T. Jarlborg, *Phys. Rev. B* **59**, 15002, (1999).
- [15] R.H. McKenzie and J.W. Wilkins, *Phys. Rev. Lett.* **69**, 1085, (1992).
- [16] F. Giustino, S.G. Louie and M.L. Cohen, *Phys. Rev. Lett.* **105**, 265501, (2010).
- [17] E. Cannuccia and A. Marini, *Phys. Rev. Lett.* **107**, 255501, (2011).
- [18] O.K. Andersen, *Phys. Rev. B* **12**, 3060, (1975).
- [19] T. Jarlborg and G. Arbman, *J. Phys. F* **7**, 1635, (1977); B. Barbiellini, S.B. Dugdale and T. Jarlborg, *Comput. Mater. Sci.* **28**, 287, (2003).
- [20] W. Kohn and L.J. Sham, *Phys. Rev.* **140**, A1133, (1965).
- [21] We adopt the same conventions as in refs. [3, 6] for the structure, site-notation and  $k$ -space, so that  $\vec{x}$  and  $\vec{z}$  are parallel and  $\vec{y}$  perpendicular to the planes.
- [22] T. Jarlborg, B. Barbiellini, H. Lin, R.S. Markiewicz and A. Bansil, *Phys. Rev. B* **84**, 045109, (2011).
- [23] C.A.M dos Santos, B.D. White, Y.-K. Yu, J.J. Neumeier and J.A. Souza, *Phys. Rev. Lett.* **98**, 266405, (2007).
- [24] M. S. da Luz, J. J. Neumeier, C. A. M. dos Santos, B. D. White, H. J. Izario Filho, J. B. Leão, and Q. Huang

- Phys. Rev. **B84**, 014108, (2011).
- [25] P. Pedrazzini, H. Wilhelm, D. Jaccard, T. Jarlborg, M. Schmidt, M. Helfland, L. Akselrud, H.Q. Yuan, U. Schwarz, Yu. Grin and F. Steglich, Phys. Rev. Lett. **98**, 047204, (2007).
- [26] G. Grimvall, *Thermophysical properties of materials*. (North-Holland, Amsterdam, 1986).
- [27] J.M. Ziman, *Principles of the Theory of Solids* (Cambridge University Press, New York, 1971).
- [28] H. Requardt, R. Currat, P. Monceau, J.E. Lorenzo, A.J. Dianoux, J.C. Lasjaunias and J. Marcus, J. Phys.: Condens. Matter **9**, 8639, (1997).
- [29] T. Jarlborg, Physica C**454**, 5, (2006).
- [30] R.E. Peierls, Quantum Theory of Solids (Oxford University, Oxford, 1955);
- [31] G. Beni and P. Pincus, J. Chem. Phys. **57**, 3531 (1972);
- [32] E. Pytte, Phys. Rev. **B10**, 4637 (1974).
- [33] T. Jarlborg, Phys. Rev. **B79**, 094530, (2009).
- [34] S. Nishimoto, M. Takahashi, and Y. Ohta, J. Phys. Soc. Jpn. **69**, 1594, (2000).
- [35] Xiaofeng Xu, A. F. Bangura, J. G. Analytis, J. D. Fletcher, M. M. French, N. Shannon, J. He, S. Zhang, D. Mandrus, R. Jin, and N. E. Hussey Phys. Rev. Lett. **102**, 206602 (2009).
- [36] J. Choi, J. L. Musfeldt, J. He, R. Jin, J. R. Thompson, D. Mandrus, X. N. Lin, V. A. Bondarenko, and J. W. Brill Phys. Rev. **B69**, 085120, (2004).
- [37] J. Chakhalian Z. Salman, J. Brewer, A. Froese, J. He, D. Mandrus, R. Jin, Physica **B359**, 361, (2005).
- [38] In ref. [9] the intensity of the upper band is much lower than of the lower one.